Composites Part B 248 (2023) 110357

Contents lists available at ScienceDirect

Composites Part B

journal homepage: www.elsevier.com/locate/composites

Hard-magnetic phenomena enable autonomous self-healing elastomers

Daniel Garcia-Gonzalez *, Tigran Ter-Yesayants, Miguel Angel Moreno-Mateos, Maria Luisa Lopez-Donaire

Department of Continuum Mechanics and Structural Analysis, Universidad Carlos III de Madrid, Avda. de la Universidad 30, 28911 Leganés, Madrid, Spain

ARTICLE INFO

Keywords:
Magnetorheological elastomers (MREs)
Self-healing
Multifunctional materials
Magneto-mechanics
Soft robotics

ABSTRACT

We propose a new concept of self-healing soft material that does not require external actuation to heal after rupture. This consists of a sticky and soft elastomeric matrix filled with hard-magnetic particles. When the material breaks into two or more parts and these are approached to each other, the magnetic particles with residual magnetisation interact closing the crack. Then, if new mechanical loading is applied, the composite acts as a continuum structure transmitting internal forces homogeneously until reaching a new failure strain threshold. We demonstrate this novel concept with experiments under tensile loading and with a magneto-mechanical constitutive model that explains the healing mechanisms. The results indicate that the proposed soft materials are able to, after several fracture cycles, sustain mechanical loading beyond 20 % strains without compromising the structural integrity. The healed material experiences no mechanical degradation during cyclic loading and healing cycles. Moreover, on its healed state, it can sustain higher stresses than the original material without residual magnetisation. We demonstrate that the strain at failure is determined by the combined effect of magnetic and adhesive contributions, which are modulated by the applied deformation rate. Furthermore, we reveal that the combination of soft and hard magnetic particles in a hybrid magnetorheological elastomer enables superior healing performance.

1. Introduction

The observation of nature opened the question on whether synthetic materials can heal external damage themselves, mimicking biological self-repairing observed in human tissues such as skin. This has motivated ground-breaking scientific works on the development of the so-called self-healing (SH) materials. These materials have the ability to heal after mechanical rupture recovering certain structural integrity. According to the healing mechanism, SH materials can be classified into extrinsic or intrinsic. Extrinsic SH materials are usually based on the encapsulation of healing agents in microcapsules [1] or vascular networks (fibres or nanotubes) [2]. Intrinsic SH materials present an inherent healing functionality and are usually based on physicochemical interactions [3] or dynamic covalent chemical bonds [4,5]. Some sophisticated solutions allow for autonomous self-healing at ambient conditions by reversible polymeric chains bonding [6–9]. However, the SH response of such materials requires significant time. When dynamic responses of these materials are required, the SH effect can be accelerated using different external energy sources such as light, conventional heating or pressure [10–13]. The main limitation of these materials is the need of an external stimulation, a point that compromises their autonomy to self-heal.

The need of external stimuli hinders the application of SH materials when these are located in confined spaces. Thus, the actuation on SH materials can be limited by the penetration depth of light or by thermal restrictions on the surrounding, i.e., non-desired heating in the neighbouring tissue or material hosting the SH structure. An alternative to partially overcome these bottlenecks consists in incorporating magnetic fillers in a polymeric matrix, so that external magnetic fields can be used to induce heating via dissipative mechanisms. In this regard, the external stimulus is an alternating magnetic field that allows for contactless, remote-controlled trigger and local actuation [14]. In addition, this solution offers extremely useful opportunities for bioengineering applications due to the low magnetic permeability of biological tissues, what enables deep actuation without perturbation of the magnetic fields [15]. Moreover, polymers with magnetic particles present further multifunctional responses related to a magneto-mechanical coupling. For example, magnetorheological elastomers (MREs) are able to mechanically deform or even change their mechanical properties (i.e., stiffness) when subjected to external magnetic fields [16,17]. Taking advantage of these functionalities, some recent works have proposed novel MREs that can respond to magnetic stimuli either mechanically stiffening under static fields; or accelerating the healing process by inductive heating under alternating fields [18,19]. In

* Corresponding author.
E-mail address: danigarc@ing.uc3m.es (D. Garcia-Gonzalez).

https://doi.org/10.1016/j.compositesb.2022.110357
Received 19 August 2022; Received in revised form 7 October 2022; Accepted 11 October 2022
Available online 21 October 2022
1359-8368/© 2022 The Author(s). Published by Elsevier Ltd. This is an open access article under the CC BY-NC-ND license (http://creativecommons.org/licenses/by-nc-nd/4.0/).

addition, some works have pushed traditional manufacturing methods of these SH MREs forward to allow the printability of such materials, opening new routes to the design of complex active structures [20–22].

Another possibility to use these MREs as SH materials consists in making use of the particle interactions to create bondings between the ruptured components. Following this idea, Cerdan et al. [23] developed elastomers that incorporated magnetite particles. After rupture, if a permanent magnet approaches the damaged region, the soft-magnetic particles interact via dipole–dipole interactions closing the crack. However, after removing the permanent magnet such a SH effect vanishes. The latter represents an important limitation as it requires the presence of a permanent magnet that, in many cases, can be highly invasive. Therefore, an open question exists on whether MREs filled with hard-magnetic particles may provide this SH functional behaviour without the need of a permanent magnet or any external activation source. Hard-magnetic particles are those that present high coercivity so that, after being subjected to a strong magnetic field, they can sustain significant magnetisation even if the external field is switched off. When adding these particles within an elastomeric matrix, they act as small permanent magnets that interact between each other and induce an internal stress state. Thus, hard-magnetic MREs have been conceived to perform a magneto-mechanical coupling that leads to complex shape changes with multiple applications [24–27]. These MREs also show significant mechanical stiffening compared to virgin samples even in the absence of external magnetic fields [28,29]. Following these ideas, [30] conceptualised exciting possibilities for conductive materials that can self-heal. However, these materials are mainly based on an electric self-healing perspective and do not provide good structural integrity.

In this work, we aim at overcoming current roadblocks in the conceptualisation of SH materials. To date, these are related to the need of an external source to activate the healing process, hindering the possibility of autonomous self-healing materials, while allowing for unlimited number of repair cycles. To this end, we propose a new concept of self-healing soft material that does not require neither external actuation nor chemical reactions to heal after rupture. This consists of a sticky ultra soft (≈1 kPa stiffness) elastomeric matrix filled with hard-magnetic particles, that are strongly magnetised during the manufacturing process. We first evaluate the effect of the magnetic-residual stresses on the mechanical behaviour of the MRE samples under uniaxial tensile loading. After rupture, we provide the mechanical response of autonomously healed MREs. The results show that our SH MREs are able to sustain large deformation beyond 20 % without fracture, and performing significant stiffening with respect to virgin samples with null pre-magnetisation. The strain at failure of these SH MREs is found to result from both the magnetic and adhesive contributions. Such contributions play different roles depending on the applied deformation rate, as the magnetic component is purely energetic and the adhesive component is highly dissipative. To isolate and elaborate on both mechanisms, we designed tests with different lubrication and pre-magnetisation conditions. Furthermore, the combination of soft and hard magnetic particles within a hybrid MRE modulates the particles interactions. This concept is demonstrated experimentally showing superior healing performance for an optimal combination of soft and hard particles. It conceptualises novel structures that can undergo large deformations and eventually self-heal, in an autonomous way and for several times without degradation. Overall, this provides exciting opportunities for applications in the bioengineering and soft-robotics fields.

2. Methods

2.1. Materials and manufacturing method

The MREs are composed of an extremely soft elastomeric matrix and micron-size magnetic particles [31,32]. The elastomeric matrix consisted of Dowsil CY52-276 (DowSil, Midland, MI, US) with two phases blended at the mixing ratio 1:1. The magnetic phase for purely hard-magnetic MREs was NdFeB powder, provided by Magnequench (MQP-S-11-9-grade powder, Neo Materials Technology Inc., Greenwood Village, Colorado, US) with a median diameter of 35–55 μm. The manufacturing of hybrid MREs also includes soft magnetic particles, i.e., SQ carbonyl iron powder (CIP) (BASF, Germany) with mean diameter 3.9–5 μm. The phases (i.e., elastomeric matrix and magnetic particles) were mixed at three different volume fractions $\phi = \{0.1, 0.2, 0.3\}$. When mixing the matrix and filler phases, the elastomeric material is pre-heated at 80 °C for 2 min to prevent sedimentation. This pre-heating increases the initial viscosity of the elastomeric component during the addition of the magnetic particles to guarantee their homogeneous distribution. Such a solution was previously adopted in recent works by the authors [29,33]. Then, two types of samples are prepared: virgin samples, i.e., MREs with null magnetisation; and magnetised samples, i.e., MREs subjected to magnetic saturation using an impulse magnetiser. Healed samples correspond to magnetised samples that reach fracture. The magnetised samples were obtained using an impulse magnetiser DXMM-12C40 Magnetiser (Dexing Magnet Tech. Co., Limited, China). More details are available in Supplemental Material.

2.2. Mechanical testing methods

Uniaxial tensile tests were performed on virgin, healed and magnetised samples. A universal testing machine was employed (INSTRON 34TM-5, INSTRON, Norwood, Massachusetts, US). To provide reliable results on the extremely soft specimens used, a 50 N load cell was employed. The gripping force was imposed by a pressure controller during the whole test to ensure non-slipping conditions and no stress concentration at these regions. The geometric design of the samples followed the UNE-EN ISO 527-2 standard. Three loading rates were tested leading to strain rates of 0.001, 0.01 and 0.1 s^{-1}. For the lubricated tests on healed samples, lubrication was applied in both fractured surfaces prior each test.

2.3. Constitutive model and implementation

To analyse the underlying mechanisms of the self-healing behaviour of the materials proposed, a microstructural-based constitutive model describes the overall response of the MRE as a mechanical contribution associated to the deformation of the elastomeric network, and another contribution arising from the magnetic interactions between particles. To this end, we define a total Helmholtz free energy function (Ψ) as the addition of mechanical (Ψ_{mech}) and magnetic (Ψ_{mag}) terms, i.e.,

$$\Psi(\mathbf{F}) = \Psi_{\text{mech}}(\mathbf{F}) + \Psi_{\text{mag}}(\mathbf{F}), \tag{1}$$

where the energetic contributions depend on the deformation gradient tensor $\mathbf{F}$. Note that the contribution due to the vacuum permeability of the free space term is assumed negligible [34]. Moreover, note that the magnetic term does not depend on a magnetic field since no external magnetic sources are applied. The mechanical potential is defined adopting a microstructural-based formulation, i.e., the eight-chain model as

$$\Psi_{\text{mech}}(\mathbf{F}) = G \sum_{k=1}^{K} \frac{C_k}{N_e^{k-1}} \left[I_1^k - 3^k \right], \tag{2}$$

where G is the shear modulus of the MRE (i.e., elastomeric matrix and particles), N_e is the number of Kuhn segments per polymer chain, and $I_1 = \text{tr}\left(\mathbf{F}^{\text{T}}\mathbf{F}\right)$. We take up to five terms in the summation that corresponds to an approximation for the inverse of the Langevin function, i.e., $\left[C_1, C_2, C_3, C_4, C_5\right] = \left[\frac{1}{2}, \frac{1}{20}, \frac{11}{1050}, \frac{19}{7000}, \frac{519}{673750}\right]$. Moreover, the magnetic energetic potential is particularised following the formulation developed by Garcia-Gonzalez and Hossain [35] for hard-magnetic MREs as

$\Psi_{\text{mag}}(\mathbf{F})$

$$= -\frac{\mu_o}{4\pi}\frac{\phi^2}{\gamma}\sum_{i=1}^{N}\left[\frac{3\left[[\mathbf{R}\mathbb{M}]\cdot\left[\mathbf{F}\mathbf{R}_i^0\right]\right]\left[[\mathbf{R}\mathbb{M}]\cdot\left[\mathbf{F}\mathbf{R}_i^0\right]\right]}{\left\|\mathbf{F}\mathbf{R}_i^0\right\|^5} - \frac{[\mathbf{R}\mathbb{M}]\cdot[\mathbf{R}\mathbb{M}]}{\left\|\mathbf{F}\mathbf{R}_i^0\right\|^3}\right], \tag{3}$$

where μ_0 is the magnetic permeability of the vacuum, $\mathbf{R}$ is the rotation tensor, $\mathbf{R}_i^0$ is a dimensionless distance between particles, and the term γ is added to account for the number of particles per representative lattice selected. The magnetisation vector $\mathbb{M}$ stands for the residual magnetisation of the hard-magnetic particles in the same direction as the applied load, i.e., longitudinal direction. Note that the MREs studied in this work enable autonomous self-healing so that no external magnetic field is needed to activate the healing process. This fact makes a difference with respect to previous works as an independent magnetic variable is not needed in the energetic potentials, and the magnetisation vector can be defined as a constant. Therefore, the total energy takes into account the mechanical resistance to deform, and the magnetic interactions between the hard-magnetic particles depending on their microstructural arrangement and their evolution during the deformation process. From this definition, the total Piola stress tensor can be derived applying the so-called Coleman–Noll argumentation, assuming incompressibility, as

$$\mathbf{P} = \frac{\partial \Omega}{\partial \mathbf{F}} - p\mathbf{F}^{-\mathbf{T}}, \tag{4}$$

where p is a Lagrange multiplier related to volumetric pressure.

The theoretical model was implemented in a MatLab script that describes the homogenised magneto-mechanical behaviour of the MRE accounting for microstructural bases. In this regard, the initial arrangement of the particles was defined via the $\boldsymbol{R}_i^0$ vectors. We considered the two limiting cases: isotropic and chain-like distributions. Then, macroscopic mechanical boundary conditions were prescribed imposing null stress in the transverse directions to the uniaxial mechanical loading. The uniaxial tensile loading was applied by prescribing the components of the macroscopic deformation gradient and assuming incompressibility conditions. The material parameters G and N_e were directly identified from experimental results on virgin samples. The calibration of the residual magnetisation $\mathbb{M}$ is not straightforward and requires the use of a homogenisation finite element model that replicates the experimental conditions and provides the $\mathbb{M}$ value in a single particle so that the MRE presents a macroscopic residual magnetic field equal to the experimental measurements (see Supplemental Material for details). The model parameters used in the simulations are collected in Table S1 (Supplemental Material).

3. Results

3.1. Hard-magnetic particles modulate the stiffness of soft MREs and enable autonomous self-healing

The residual magnetisation offered by hard-magnetic particles within a soft elastomeric matrix is envisaged here as a potential source of autonomous healing. When magnetised, these particles experience attraction forces that, under rupture conditions, promote the closure of cracks. This idea is tested on MREs composed of an extremely soft elastomer (≈ 1 kPa) filled with hard-magnetic fillers at different volume ratios (see Methods). First, virgin and magnetised MRE samples with different volume fractions were tested under uniaxial tensile loading and quasi-static conditions (see Methods). Fig. 1 depicts the results in terms of Cauchy stress versus logarithmic strain. The permanent magnetisation in the magnetised samples induces internal stresses that lead to material stiffening. This indicates that the magnetic forces are the main contributor to healing. This stiffening becomes higher with the particle volume content, showing a maximum increase in Young's modulus of > 4.5 times for 30 % volume fraction (see Fig. 1). Moreover, no significant differences were appreciated on the strain at failure. The major question of these tests is whether the particle interactions between two pieces of magnetised samples after breakage are able to close the main crack and provide structural integrity during a second loading. To answer this question, we defined "healed" samples consisting of the two resulting pieces of magnetised samples that, after rupture, are put together. When doing so, both broken parts act as permanent magnets attracting each other and generating an interacting force that heals the fracture. Then, a uniaxial test is performed on these samples until reaching new rupture. Fig. 1 shows the results along with the corresponding ones for virgin and magnetised samples.

The experimental findings suggest that the healed samples are able to sustain higher stresses than the virgin material and very close to the magnetised samples up to a strain threshold that depends on the magnetic filler content. This strain threshold is 10.5 %, 13.5 % and 21.1 % for particle volume ratios of 10 %, 20 % and 30 %, respectively. Although the strain after failure is significantly smaller than the strain of the material before failure (above 100 % strain), note that the working strain range is sufficient to enable many different applications, e.g., sensors whose failure strain can be tuned by the material composition. The stiffness of the healed samples is almost equivalent to the magnetised samples and significantly higher than the virgin ones (Fig. 1D), which suggests that their structural integrity up to failure is partly provided by the magnetic stress component. However, the sticky nature of the elastomeric matrix is another source of structural integrity. It must be noted that the response of the healed samples has been observed for healing-loading cycles without loss in the mechanical behaviour (we tested up to 10 cycles). The similarity between the stiffness moduli of the pre-magnetised and healed samples indicates that there is almost no degradation of the mechanical properties during the healing cycles. This behaviour is further illustrated in Fig. 2, where the testing stages of the stress–strain response are accompanied by experimental pictures of the healing and rupture processes. Herein, the healing process can be observed when the two broken pieces of the tested magnetised sample are approached. Note that the process does not need any external energetic source and occurs instantaneous and autonomously. Then, if another tensile loading is applied, the material is able to transmit the internal stresses within the whole structure until reaching large deformations beyond 20 % in true strain.

3.2. The balance between magnetic stress from dipole–dipole interactions and mechanical stress from polymeric network determines the rupture threshold of healed samples

The extremely soft hard-magnetic MREs developed herein provide unlimited autonomous self-healing cycles. This capacity depends on the relation between the mechanical properties of the elastomeric matrix, the amount of particles and their remanent magnetisation, which determines the resultant interactive forces. These variables determine the self-healing properties of the MREs and the strain threshold that leads to fracture. To deepen into this concept, we make use of the microstructural-based constitutive model described in Methods section. The overall mechanical response of the MRE is understood as a purely mechanical contribution associated to the deformation of the elastomeric network, and another contribution from dipole–dipole magnetic interactions between particles. The proposed theoretical framework can be used to design the failure strain of the healed samples from the material properties of the composite phases (i.e., elastomeric matrix and particles used). To illustrate this, Fig. 3A shows model predictions for the MRE studied with 30 % of particles volume fraction. The stress–strain curves here represent the model predictions of the mechanical and magnetic contributions to the total material stress during tensile loading. Note that the particles are isotropically distributed in the virgin samples but, after the pre-magnetisation, they are expected to rearrange at certain extent forming chain-like structures. Therefore, we represent the magnetic contribution that corresponds to both extreme cases. The analysis of the modelling results suggests a strong magnetic contribution due to dipole–dipole interactions between particles at low

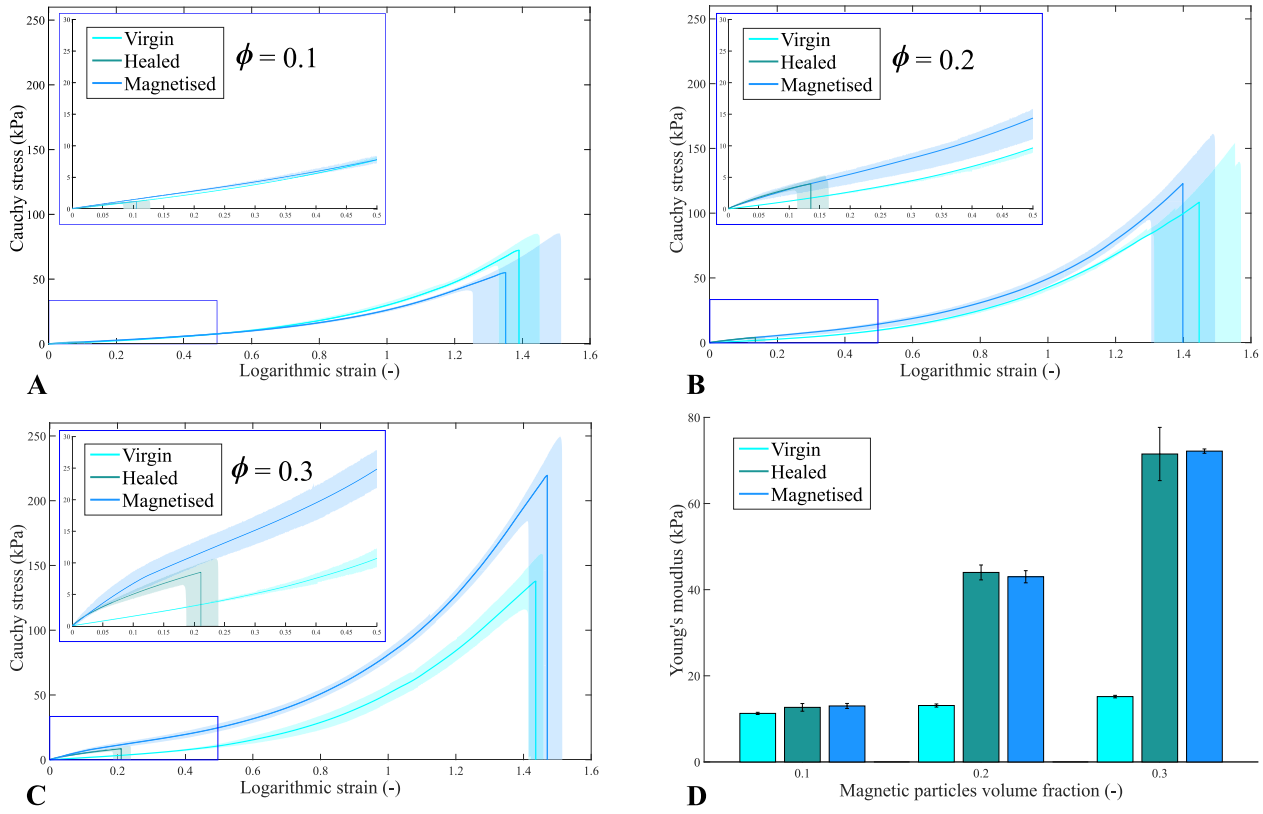


Fig. 1. Experimental results on virgin, healed and magnetised samples subjected to quasi-static uniaxial tensile loading. (A), (B) and (C) present the Cauchy stress versus logarithmic strain for MREs with particle volume ratio of 10 %, 20 % and 30 %, respectively. The shaded regions indicate experimental dispersion. (C) Mean Young's modulus and standard deviation of virgin, healed and magnetised MRE samples with different volume ratios. The healed samples perform better, in terms of stiffness, than the virgin samples and close to magnetised samples.

strains. At such a low deformation, the polymeric chains are not aligned leading to low mechanical stress contribution. Therefore, during this deformation stage, the magnetic stress governs the problem and the strains can be distributed homogeneously within the sample. However, larger strains promote two main events: (i) an increase in the relative distance between particles, decreasing the dipole–dipole interactions and thus the magnetic stress contribution; and (ii) the alignment of the polymeric network along the loading direction increasing the mechanical stress contribution. Hence, at a given strain threshold, which corresponds to the crosspoint between magnetic and mechanical stress contributions, the mechanical resistance becomes the main player. As a consequence, the sample deformation focuses within the original rupture region resulting in the breakage of the material. However, if the two broken pieces are put together again, the dipole–dipole interaction would increase leading to the initial state of the healed sample. This process is schematically explained in Fig. 3C. Without further calibration, the model is tested to provide an estimation of the failure strain for the different particle volume fractions. Fig. 3B presents the results. These show a good qualitative agreement between experiments and model predictions, although the model predictions present higher deviation at lower particle volume fractions. This is explained by the mechanical resistance from adhesive forces within the contact surfaces of the broken pieces, which are neglected in the theoretical approach. These have a higher influence in the low volume fraction cases where the magnetic contribution is weaker. A deeper analysis of this phenomenon is presented next, reconciling the experimental results with the model predictions.

3.3. The combined effect of adhesive forces and magnetic stress modulates the strain at failure of healed samples depending on the deformation rate

The experimental results shown in Fig. 3B for low particles volume fractions are not in good agreement with the theoretical strain thresholds leading to rupture in healed samples. This observation suggests that the magnetic interaction between particles is not the only player in the healing process. Complementing this mechanism there are adhesive forces between the broken pieces of the healed sample due to the sticky nature of the elastomeric matrix used. Here, we devise an experimental procedure to isolate and characterise both healing mechanisms. To this end, we conduct tensile tests on healed samples under three main conditions: (1) virgin healed samples with no pre-magnetisation to isolate the adhesive forces of the matrix, i.e., virgin samples that, after rupture, are joined together making use of the sticky nature of the elastomeric matrix; (2) lubricated healed samples to isolate the magnetic forces, i.e., magnetised healed samples that are lubricated within the fracture region so that adhesive forces are removed; (3) regular healed samples with both adhesive and magnetic forces, i.e., magnetised healed samples without lubricant (as used in the previous results). In addition, these tests are carried out for three different strain rates. The motivation for testing different deformation rates lies in the nature of the healing mechanisms. In this regard, the magnetic forces depend on the relative position of the magnetic particles within the MRE and do not present significant dissipative contributions [36]. However, the adhesive forces are highly dissipative. Therefore, a strong rate dependence in the adhesive contribution is presumed whereas this dependence is expected to be negligible for the magnetic contribution.

The results for these tests are presented in Fig. 4. We conducted tests on elastomeric samples without magnetic particles to provide a clear picture of the effect of adhesive forces on the strain at failure, Fig. 4A–B. The strain at failure strongly depends on the deformation rate applied, increasing the former with the latter. The stresses transmitted within the MRE under these conditions are very low compared with the stress magnitudes shown by magnetised healed samples. These effects are, therefore, intimately associated to the elastomeric matrix

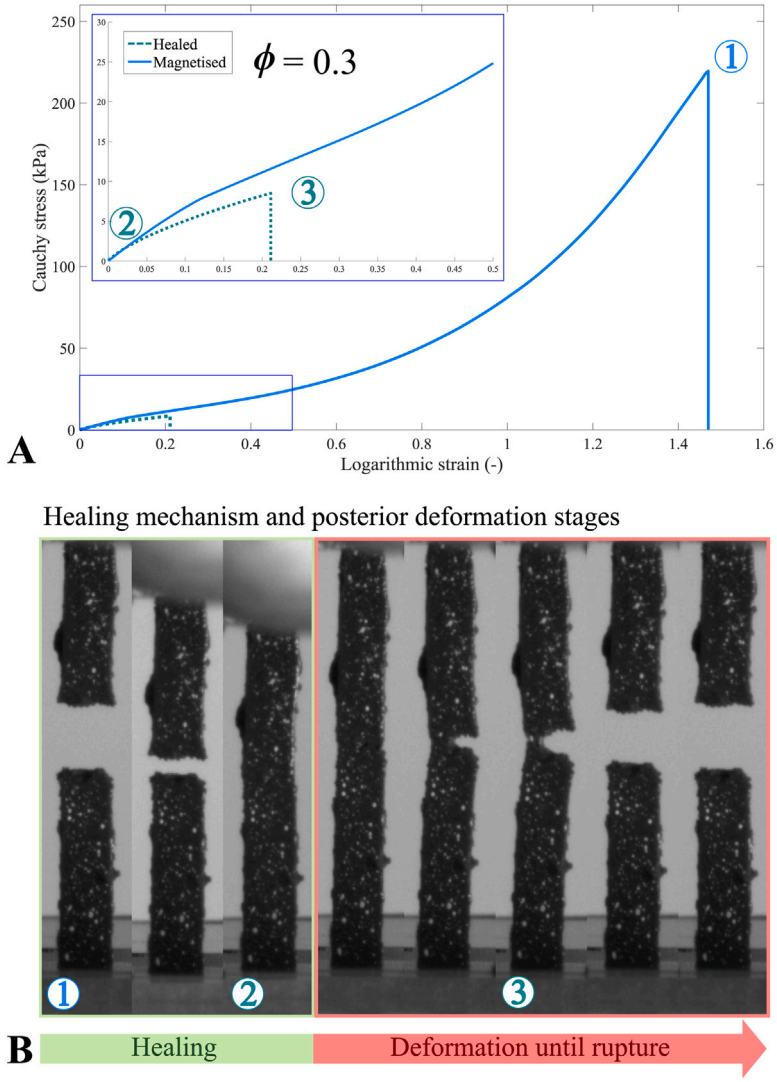


Fig. 2. (A) Comparison of the stress–strain experimental results on magnetised and healed (magnetised and healed after rupture) samples. (B) Experimental pictures of the healing and deformation processes. The first stage of the healing process, indicated with (1), corresponds to the rupture point of a magnetised sample (see point (1) in panel A). When approaching both broken parts, the magnetic interaction actuates healing the sample and removing the crack. This healed condition, indicated with (2), corresponds to the initial stage of the healed sample (see point (2) in panel A). When applying a mechanical load on this sample, i.e., deformation until rupture, a homogeneous deformation is transmitted through the whole sample until reaching a threshold where the mechanical resistance is predominant over the magnetic resistance and the sample breaks (see point (3) in both panels A and B).

embedding the fillers. In this regard and when adding the particles, the higher volume fraction, the bigger effective surface occupied by the elastomeric matrix and, subsequently, the lower strain at failure. Moreover, the tests on lubricated healed samples provide a clear picture of the effects of magnetic forces on the strain at failure, Fig. 4C–E. In this regard, a strong direct dependence of the particle volume fraction on this variable is observed. This is due to the increase in dipole–dipole interactions that results in a stronger force between the two parts that compose the sample. Moreover, no relevant differences in the strain at failure are appreciated when varying the strain rate conditions. Note that the offset at the highest rate can be attributed to the sensibility of the testing device. In this regard, to confirm the independence of the strain to failure of lubricated samples on the strain rate, we report additional tests in Supplemental Material for strain rates lower than 0.001 s^{-1}. In addition, a slight increase in stress values is obtained when increasing the strain rate. This indicates the capability of the healed material to transmit the stresses/strains within the whole sample incorporating the mechanical resistance of the elastomeric matrix, that presents moderate hardening with strain rate (see a previous work on the same matrix [32]). Moreover, note that in some cases (e.g., Fig. 4.E) the stiffness modulus for the lubricated case is slightly larger than the modulus for the non-lubricated case. This may arise from the stickiness of the material and the quality of the fracture interface. For the lubricated samples, the removal of the stickiness allows us to place both surfaces perfectly aligned. However, when not using the lubricant, the placement is not perfect, hence the contact and alignment of both surfaces are not optimal leading to the observed response.

The final tests were conducted on magnetised healed samples at different strain rates, Fig. 4C–E. These results show that there is a mechanistic competition between magnetic and adhesive forces that determines the strain thresholds leading to fracture. In this regard, the magnetic contribution establishes a rate-independent threshold that is defined by the amount of particles and their residual magnetisation. Moreover, the nature of the elastomeric matrix defines the adhesive contribution that is highly sensitive on strain rate. Therefore, it determines a rate-dependent threshold. Then, for a given sample and testing condition, the failure strain is specified by the maximum of the magnetic and adhesive thresholds. This explanation is consistent with all the results presented herein. Finally, the comprehension of these mechanisms allows for concealing the differences between experiments and

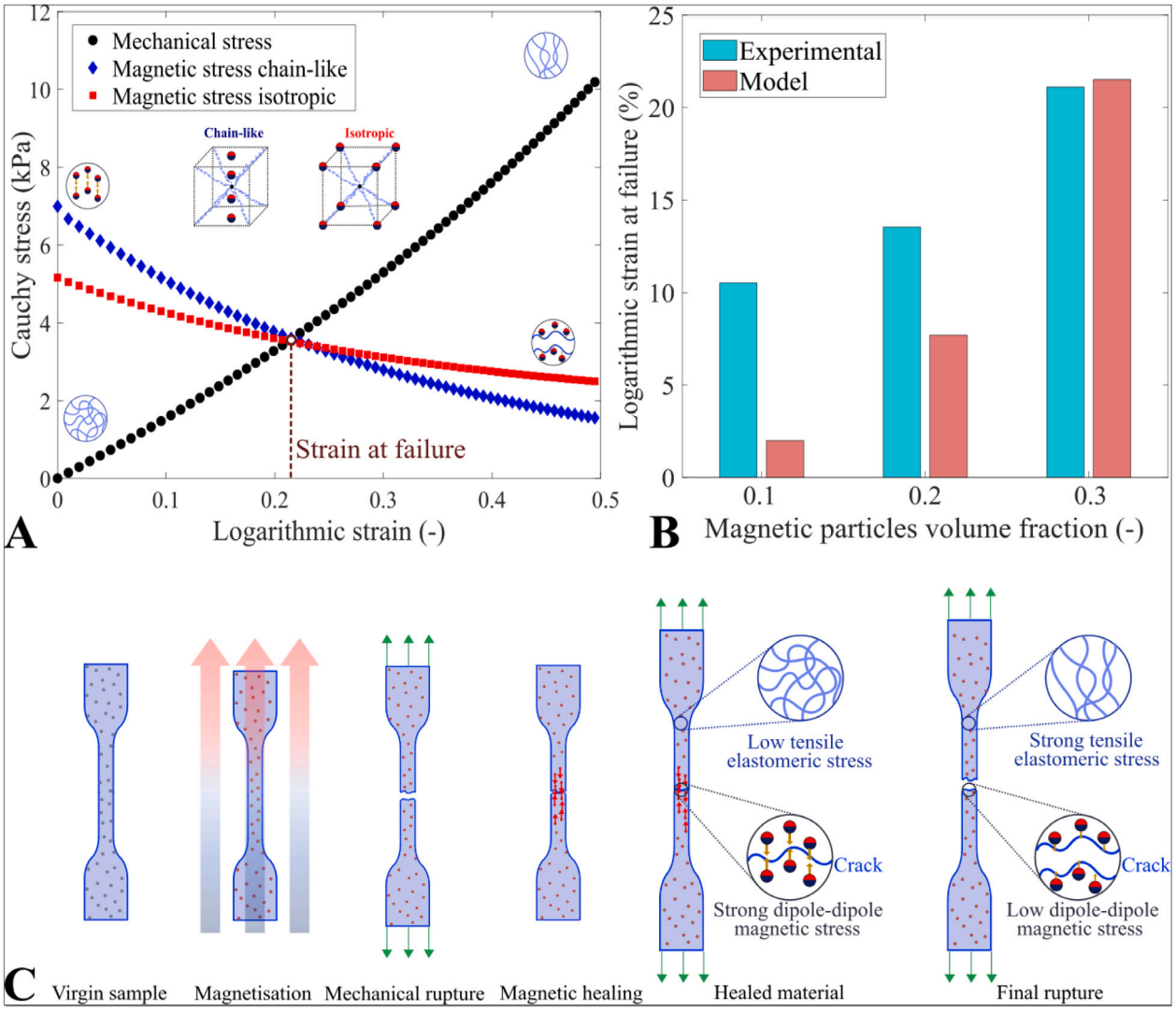


Fig. 3. (A) Evolution of mechanical and magnetic stress components in the MRE composite according to theoretical simulations, for a particle volume fraction of 30 %. (B) Comparison between experimental results and theoretical simulations in terms of strain at failure depending on the magnetic particles volume fraction. (C) Scheme of the autonomous self-healing idea. A virgin sample consisting of a soft elastomeric matrix filled with hard-magnetic particles can be magnetised upon magnetic saturation. Then, the material can be deformed until fractured. When approaching both broken parts, the magnetised particles interact via dipole-to-dipole interactions closing the crack and, thus, "healing" the material. Then, if new mechanical loading is applied, the material undergoes homogeneous mechanical deformation until reaching a threshold where the mechanical stress becomes predominant over the magnetic stress leading to new rupture.

the theoretical predictions. Fig. 4F presents the comparison, by means of strain at failure, between the experiments on lubricated healed samples and theoretical predictions, showing a good agreement in both qualitative and quantitative terms. This proves the validity of the theoretical framework presented to design the magnetic strain-threshold of healed samples.

3.4. The combination of soft and hard magnetic particles enables superior healing performance

In a recent article by the authors [33], we demonstrated that the appropriate combination of soft and hard magnetic particles within an ultra-soft polymeric matrix opens new routes to design versatile multifunctional actuators. Motivated by this concept, here we explore whether the microstructural interaction between both types of particles may result in a superior healing performance. To this end, we manufacture hybrid MREs containing a total filler volume fraction of 30 % and considering soft-to-hard magnetic particles mixing ratios of 0:1 (previous results), 1:2, 1:1 and 2:1 (see Fig. 5A). Then, we conduct uniaxial tensile tests on virgin, magnetised and healed samples following the same procedure as in Fig. 1. These results are shown in Fig. 5B–D. For a quantitative comparison we take the logarithmic strain at failure as the representative variable, Fig. 5E. The strain at failure, as discussed previously, is determined by the combined effect of mechanical and magnetic stress contributions. We report herein a significant superior performance for the 1:2 hybrid MRE, with a larger strain at failure of 38 % than that for the pure hard magnetic MRE. This result is not obvious as one may expect higher strains at failure for higher hard-magnetic content, because these particles are the responsible to provide a remanent magnetic field and the self-healing mechanism. However, as explained numerically in a previous work [33], the combination of soft and hard particles leads to synergistic magneto-mechanical interactions. In this regard, hard particles contribute to remanent fields [37] whereas soft particles amplify the magnetisation by creating magnetic bridges. Hence, the dipole–dipole interactions are amplified allowing larger sample deformations before rupture. This concept also adds new variables for designing purposes to modulate both mechanical and magnetic properties.

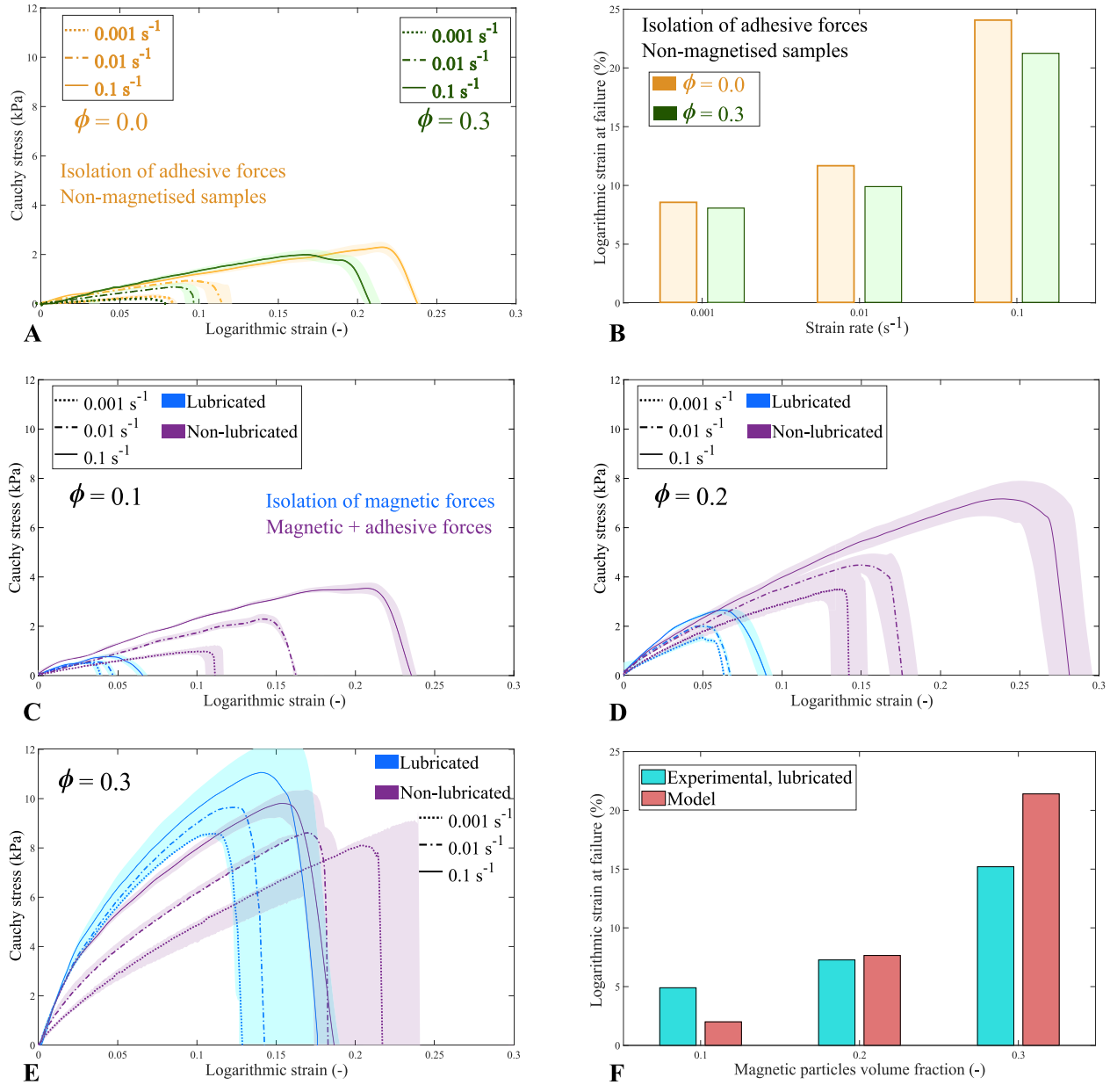


Fig. 4. (A) Experimental Cauchy stress versus logarithmic strain on elastomeric samples, i.e., no magnetic particles embedded, and with particle volume ratio of 30 % subjected to uniaxial tensile loading at different strain rates: 0.001, 0.01 and 0.1 s^{-1}. (B) Experimental results on elastomeric samples and with particle volume ratio of 30% representing the mean strain at failure versus strain rate. See Supplemental Material for results on 10 and 20% volume ratios. (C), (D) and (E) present the Cauchy stress versus logarithmic strain for healed MRE samples with particle volume ratio of 10 %, 20 %, and 30 %, respectively. These results are shown for both lubricated and non-lubricated samples. The shaded regions indicate experimental dispersion. (F) Comparison between experimental results and theoretical simulations in terms of strain at failure depending on the magnetic particles volume fraction. The experimental results correspond to lubricated healed samples.

4. Discussion and conclusions

We have conceptualised MREs that provide autonomous self-healing properties without the need of an external energetic source. This is achieved by the combination of an sticky elastomeric matrix and hard-magnetic particles that present residual magnetisation. The healing properties arise from two main contributions: magnetic particle interactions and adhesive forces. Unlike other approaches in the literature, this SH response is independent of the healing cycles, providing a stable behaviour over time and loading conditions. However, although the magnetic contribution is independent of rate loading conditions, the dissipative nature of the adhesive forces introduces a rate dependence with the deformation rate. We demonstrated that the rate-independent contribution associated to the magnetic forces can be predicted by a microstructural-based constitutive model. The effectiveness of the healing depends on the nature of the matrix (i.e., compliance to mechanically deform) and on the nature of the magnetised particles. The range of applicability is, therefore, a two-variable space. In this regard, the proposed theoretical framework can be used to evaluate and design the strain threshold leading to fracture of the healed material. To this end, the remanent magnetisation of the particles and the stiffness of the MRE, as well as their relative volume fraction, are the input parameters to be tuned. Note that low particles content or high matrix stiffness will significantly reduce the strain at failure of the material. Therefore, effective self-healing properties are expected for significant particle volume fractions and soft polymeric matrices. Moreover, we provide

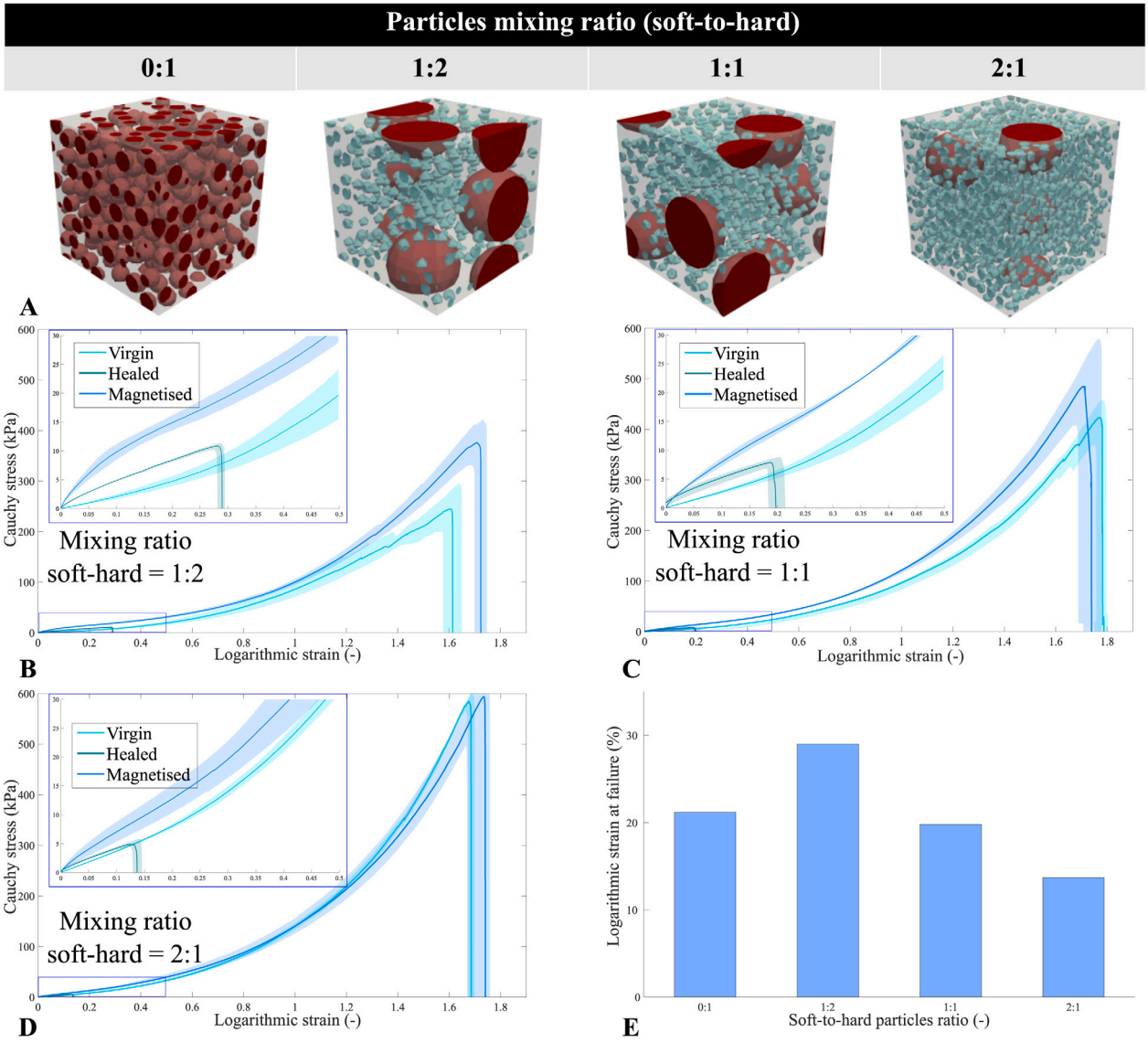


Fig. 5. Experimental results on hybrid MREs for different soft-to-hard particles mixing ratios. (A) Representative scheme of the mixing ratios considered: 0:1 (pure hard-magnetic), 1:2, 1:1 and 2:1. Red particles represent hard-magnetic and blue particles represent soft magnetic ones. (B), (C), (D) present the experimental results on virgin, healed and magnetised samples subjected to quasi-static uniaxial tensile loading for hybrid MREs with particles mixing ratios of 1:2, 1:1 and 2:1, respectively. The shaded regions indicate the experimental dispersion. (E) Mean logarithmic strain at failure of healed samples with different mixing ratios. The hybrid MREs with a 1:2 mixing ratio perform significantly better than purely hard-magnetic MREs. All hybrid MREs present a total filler volume fraction of 30 %.

an experimental methodology to characterise the adhesive forces due to the sticky elastomeric matrix and their effect on the rate-dependence of the failure strain.

The combination of these magnetic and adhesive contributions opens great opportunities for designing sensor–actuator systems driven by a "rupture strain threshold" that can be designed to depend on the deformation rate. This concept is especially relevant for applications where binary conditions are needed based on a mechanical threshold. In this regard, we provide additional experiments in Fig. 6 which demonstrate that the remanent magnetisation provides healed materials whose properties do not degrade during the loading cycles. Therefore, the proposed healed material presents mechanical properties that do not degrade during loading until reaching failure, and that can be fully recovered after fracture for several healing cycles. A schematic representation of the proposed material used as programmed strain sensors is shown in Fig. 6. A potential application that can benefit from this SH material is the development of microfluidic membranes. Note that the proposed materials can work in the presence of high humidity or even underwater, which is an important distinction with respect to many solutions in the literature. These devices can act as a barrier for a given fluid and, when a mechanical threshold due to an increase in pressure or volume is reached, the prescribed crack will open allowing for fluid flow through the membrane. Then, if the pressure decreases below the given threshold, the membrane will recover its original shape elastically resulting in the recovery of the strong magnetic interactive forces, allowing for another actuation cycle. Another interesting application field is soft electronics. If conductive particles are added to the matrix, these materials would allow for conductive conditions during the deformation process leading to abrupt changes in conductance when reaching failure conditions. Therefore, signals based on a specific strain threshold and a binary stiffness (i.e., mechanical resistance or null resistance) could be obtained over several cycles. However, the reprocessing of these applications with elastomers is still a challenge. The capability to self-heal may make them compatible with the circular economy model allowing for reducing waste and extending their lifetime [38].

To support the design of such applications, the theoretical and experimental methods presented herein are essential. The development

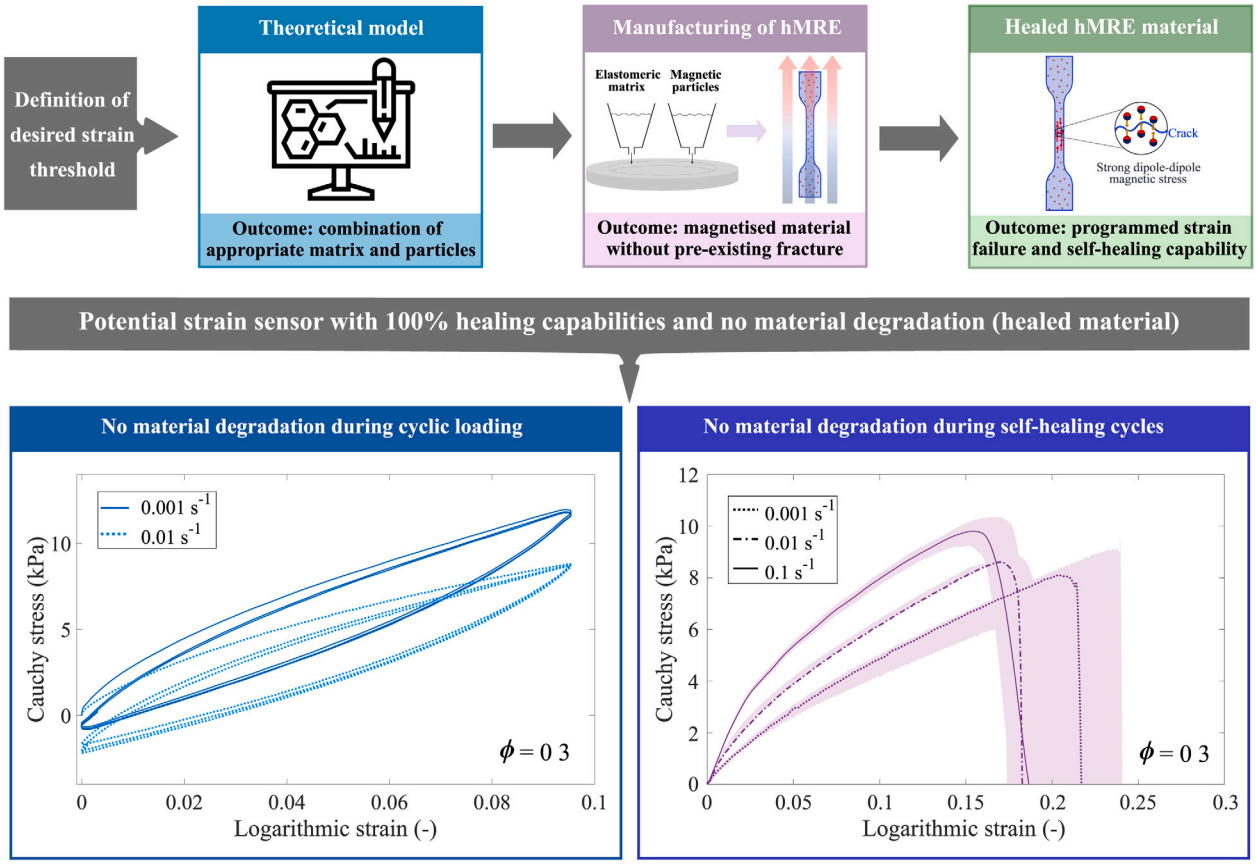


Fig. 6. Scheme for the conceptualisation and design of strain-based sensors: (1) a desired strain threshold is defined; (2) the theoretical model can be used to obtain, by inverse engineering approaches, the optimal material composition; (3) hMRE with a given shape can be manufactured according to the material composition predicted and magnetised until saturation; (4) the final samples are cut at a given location and the two pieces are approached each other resulting in the healed sample. These healed samples provide no material degradation during cyclic conditions and during self-healing cycles.

of rate-independent sensor–actuator systems based on strain thresholds is straightforward using lubricated samples or non-sticky elastomeric matrices. The strain threshold can be designed by making use of the theoretical model proposed. To this end, the theoretical framework can be employed to virtually test the combination of different alternatives for the elastomeric and filler phases. Then, the optimal solutions obtained can be easily tested with the tensile tests presented in Fig. 4 for validation purposes. Moreover, the development of finite element frameworks based on micromechanics and homogenised models would help optimise parameters such as the soft-hard particles' mixing ratio. These frameworks would account for the rearrangement of the particles along the deformation process. Although such approaches would be more precise, they would increase the computational cost. Therefore, at this stage, we conceive the proposed modelling framework as a first powerful tool to understand the fundamentals of the self-healing phenomena and as a fast virtual testing framework to evaluate the self-healing effectiveness. Overall, the development of rate-dependent sensor–actuator systems needs further efforts. The theoretical approach requires complementary experiments to characterise the effect of the adhesive forces. In this case, tensile tests on non-magnetised (virgin) samples would be necessary to understand the rate effects on the strain at failure.

Future improvement would consider the pre-arrangement of magnetic particles forming chain-like structures along the actuation direction. This can be achieved by imposing an external magnetic field during the curing process of the MRE and would allow to control anisotropic mechanical properties of the material as well as to reinforce the magnetic interactions. Consequently, it would enable for a superior self-healing performance. In the case that there is a deviation between the load direction and the pre-magnetisation of the MRE, the healing effectiveness would be worse. However, such a loading condition would not be of interest for functional applications. From the numerical perspective, the designing process of these materials would greatly benefit from the development of finite element frameworks to model the magneto-mechanical problem. These approaches would permit the consideration of geometrical effects on the healing process and the numerical study of heterogeneous deformations within the sample.

Overall, the hard-magnetic materials presented herein open new possibilities for soft sensors based on mechanical inputs. Our solution can be conceived as complementary to other approaches such as self-healing materials based on hydrogen bonding [39–42]. Hydrogen bonding-based methods provide significantly larger deformation ranges and stiffer responses under healed conditions. However, our material provides identical self-healing efficiency independently of the healing cycle, and instantaneous self-healing reaching the maximum healing capacity almost instantaneously. Furthermore, under scenarios with no strong external magnetic fields, our approach is independent of the environmental conditions, i.e., presence of water or other solvents, which can be an issue for certain hydrogen bonding-based approaches [43].

CRediT authorship contribution statement

Daniel Garcia-Gonzalez: Conceptualisation, Investigation, Experimental methodology, Computational methodology, Formal analysis, Writing – original draft, Writing – review & editing, Funding acquisition. **Tigran Ter-Yesayants:** Experimental methodology, Writing – review & editing. **Miguel Angel Moreno-Mateos:** Investigation, Computational methodology, Formal analysis, Writing – review & editing. **Maria Luisa Lopez-Donaire:** Investigation, Experimental methodology, Formal analysis, Writing review & editing.

Declaration of competing interest

The authors declare the following financial interests/personal relationships which may be considered as potential competing interests: Daniel Garcia-Gonzalez has patent Material conductivo autorreparable pending to ES3473.14.

Data availability

Data will be made available on request.

Acknowledgements

The authors acknowledge support from the European Research Council (ERC) under the European Union's Horizon 2020 research and innovation programme (grant agreement No. 947723, project: 4D-BIOMAP). DGG acknowledge support from MCIN/ AEI/10.13039/501100011033 under Grant number PID2020-117894GA-I00. MAMM acknowledges support from the Ministerio de Ciencia, Innovacion *y* Universidades, Spain (FPU19/03874). DGG acknowledges support from the Talent Attraction grant (CM 2018 - 2018-T2/IND-9992) from the Comunidad de Madrid.

Appendix A. Supplementary data

Supplementary material related to this article can be found online at https://doi.org/10.1016/j.compositesb.2022.110357.

References

[1] Samadzadeh M, Boura SH, Peikari M, Kasiriha S, Ashrafi A. A review on self-healing coatings based on micro/nanocapsules. Prog Org Coat 2010;68(3):159–64, URL https://www.sciencedirect.com/science/article/pii/S030094401000024X.

[2] Cuvellier A, Torre-Muruzabal A, Van Assche G, De Clerck K, Rahier H. Selection of healing agents for a vascular self-healing application. Polym Test 2017;62:302–10, URL https://www.sciencedirect.com/science/article/pii/S0142941817306852.

[3] Herbst F, Döhler D, Michael P, Binder WH. Self-healing polymers via supramolecular forces. Macromol Rapid Commun 2013;34(3):203–20, arXiv:https://onlinelibrary.wiley.com/doi/pdf/10.1002/marc.201200675, URL https://onlinelibrary.wiley.com/doi/abs/10.1002/marc.201200675.

[4] Wojtecki RJ, Meador MA, Rowan SJ. Using the dynamic bond to access macroscopically responsive structurally dynamic polymers. Nature Mater 2011;10(1):14–27. http://dx.doi.org/10.1038/nmat2891.

[5] Wu J, Cai L-H, Weitz DA. Tough self-healing elastomers by molecular enforced integration of covalent and reversible networks. Adv Mater 2017;29(38):1702616, arXiv:https://onlinelibrary.wiley.com/doi/pdf/10.1002/adma.201702616, URL https://onlinelibrary.wiley.com/doi/abs/10.1002/adma.201702616.

[6] Cordier P, Tournilhac F, Soulié-Ziakovic C, Leibler L. Self-healing and thermoreversible rubber from supramolecular assembly. Nature 2008;451(7181):977–80. http://dx.doi.org/10.1038/nature06669.

[7] Chen Y, Kushner AM, Williams GA, Guan Z. Multiphase design of autonomic self-healing thermoplastic elastomers. Nature Chem 2012;4(6):467–72. http://dx.doi.org/10.1038/nchem.1314.

[8] Guo H, Han Y, Zhao W, Yang J, Zhang L. Universally autonomous self-healing elastomer with high stretchability. Nature Commun 2020;11(1):2037. http://dx.doi.org/10.1038/s41467-020-15949-8.

[9] Zhang Z, Ghezawi N, Li B, Ge S, Zhao S, Saito T, et al. Autonomous self-healing elastomers with unprecedented adhesion force. Adv Funct Mater 2021;31(4):2006298. http://dx.doi.org/10.1002/adfm.202006298, arXiv:https://onlinelibrary.wiley.com/doi/pdf/10.1002/adfm.202006298, URL https://onlinelibrary.wiley.com/doi/abs/10.1002/adfm.202006298.

[10] Burnworth M, Tang L, Kumpfer JR, Duncan AJ, Beyer FL, Fiore GL, et al. Optically healable supramolecular polymers. Nature 2011;472(7343):334–7. http://dx.doi.org/10.1038/nature09963.

[11] Wu S, Li J, Zhang G, Yao Y, Li G, Sun R, et al. Ultrafast self-healing nanocomposites via infrared laser and their application in flexible electronics. ACS Appl Mater Interfaces 2017;9(3):3040–9. http://dx.doi.org/10.1021/acsami.6b15476.

[12] Hong G, Zhang H, Lin Y, Chen Y, Xu Y, Weng W, et al. Mechanoresponsive healable metallosupramolecular polymers. Macromolecules 2013;46(21):8649–56. http://dx.doi.org/10.1021/ma4017532.

[13] Qu P, Lv C, Qi Y, Bai L, Zheng J. A highly stretchable, self-healing elastomer with rate sensing capability based on a dynamic dual network. ACS Appl Mater Interfaces 2021;13(7):9043–52. http://dx.doi.org/10.1021/acsami.1c00282.

[14] Hohlbein N, Shaaban A, Schmidt A. Remote-controlled activation of self-healing behavior in magneto-responsive ionomeric composites. Polymer 2015;69:301–9, URL https://www.sciencedirect.com/science/article/pii/S003238611500350X.

[15] Son D, Ugurlu MC, Sitti M. Permanent magnet array–driven navigation of wireless millirobots inside soft tissues. Sci Adv 2021;7(43):eabi8932, arXiv:https://www.science.org/doi/pdf/10.1126/sciadv.abi8932, URL https://www.science.org/doi/abs/10.1126/sciadv.abi8932.

[16] Moreno-Mateos MA, Gonzalez-Rico J, Nunez-Sardinha E, Gomez-Cruz C, Lopez-Donaire ML, Lucarini S, et al. Magneto-mechanical system to reproduce and quantify complex strain patterns in biological materials. Appl Mater Today 2022;27:101437, URL https://www.sciencedirect.com/science/article/pii/S2352940722000762.

[17] Danas K, Kankanala S, Triantafyllidis N. Experiments and modeling of iron-particle-filled magnetorheological elastomers. Journal of the Mechanics and Physics of Solids 2012;60(1):120–38. http://dx.doi.org/10.1016/j.jmps.2011.09.006, https://www.sciencedirect.com/science/article/pii/S0022509611001736.

[18] Wang Y, Ding L, Zhao C, Wang S, Xuan S, Jiang H, et al. A novel magnetorheological shear-stiffening elastomer with self-healing ability. Compos Sci Technol 2018;168:303–11, URL https://www.sciencedirect.com/science/article/pii/S0266353818309679.

[19] Ding L, Zhang S, Wang Q, Wang Y, Xuan S, Gong X, et al. Self-healing and printable elastomer with excellent shear stiffening and magnetorheological properties. Compos Sci Technol 2022;223:109430, URL https://www.sciencedirect.com/science/article/pii/S0266353822001725.

[20] Qi S, Fu J, Xie Y, Li Y, Gan R, Yu M. Versatile magnetorheological plastomer with 3D printability, switchable mechanics, shape memory, and self-healing capacity. Compos Sci Technol 2019;183:107817, URL https://www.sciencedirect.com/science/article/pii/S0266353819320950.

[21] Yu K, Xin A, Du H, Li Y, Wang Q. Additive manufacturing of self-healing elastomers. NPG Asia Mater 2019;11(1):7. http://dx.doi.org/10.1038/s41427-019-0109-y.

[22] Nardecchia S, Jiménez A, Morillas JR, de Vicente J. Synthesis and rheological properties of 3D structured self-healing magnetic hydrogels. Polymer 2021;218:123489, URL https://www.sciencedirect.com/science/article/pii/S0032386121001129.

[23] Cerdan K, Van Assche G, van Puyvelde P, Brancart J. A novel approach for the closure of large damage in self-healing elastomers using magnetic particles. Polymer 2020;204:122819, URL https://www.sciencedirect.com/science/article/pii/S0032386120306479.

[24] Kim Y, Yuk H, Zhao R, Chester SA, Zhao X. Printing ferromagnetic domains for untethered fast-transforming soft materials. Nature 2018;558(7709):274–9. http://dx.doi.org/10.1038/s41586-018-0185-0.

[25] Lucarini S, Hossain M, Garcia-Gonzalez D. Recent advances in hard-magnetic soft composites: Synthesis, characterisation, computational modelling, and applications. Compos Struct 2022;279:114800, URL https://www.sciencedirect.com/science/article/pii/S0263822321012460.

[26] Mukherjee D, Rambausek M, Danas K. An explicit dissipative model for isotropic hard magnetorheological elastomers. Journal of the Mechanics and Physics of Solids 2021;151:104361. http://dx.doi.org/10.1016/j.jmps.2021.104361, https://www.sciencedirect.com/science/article/pii/S0022509621000569.

[27] Zhang Q, Rudykh S. Magneto-deformation and transverse elastic waves in hard-magnetic soft laminates. Mechanics of Materials 2022;169:104325. http://dx.doi.org/10.1016/j.mechmat.2022.104325, https://www.sciencedirect.com/science/article/pii/S0167663622001041.

[28] Stepanov GV, Borin DY, Bakhtiiarov AV, Lobanov DA, Storozhenko PA. Ring-like structures in magnetoactive elastomers based on magnetic hard powder. Smart Mater Struct 2020;30(1):015023. http://dx.doi.org/10.1088/1361-665x/abca82.

[29] Moreno-Mateos MA, Lopez-Donaire ML, Hossain M, Garcia-Gonzalez D. Effects of soft and hard magnetic particles on the mechanical performance of ultra-soft magnetorheological elastomers. Smart Mater Struct 2022. URL http://iopscience.iop.org/article/10.1088/1361-665X/ac6bd3.

[30] Bandodkar AJ, López CS, Mohan AMV, Yin L, Kumar R, Wang J. All-printed magnetically self-healing electrochemical devices. Sci Adv 2016;2(11):e1601465, arXiv:https://www.science.org/doi/pdf/10.1126/sciadv.1601465, URL https://www.science.org/doi/abs/10.1126/sciadv.1601465.

[31] Pathak P, Arora N, Rudykh S. Magnetoelastic instabilities in soft laminates with ferromagnetic hyperelastic phases. International Journal of Mechanical Sciences 2022;213:106862. http://dx.doi.org/10.1016/j.ijmecsci.2021.106862, https://www.sciencedirect.com/science/article/pii/S002074032100583X.

[32] Moreno MA, Gonzalez-Rico J, Lopez-Donaire M, Arias A, Garcia-Gonzalez D. New experimental insights into magneto-mechanical rate dependences of magnetorheological elastomers. Composites B 2021;224:109148, URL https://www.sciencedirect.com/science/article/pii/S1359836821005291.

[33] Moreno-Mateos MA, Hossain M, Steinmann P, Garcia-Gonzalez D. Hybrid magnetorheological elastomers enable versatile soft actuators. Npj Comput Mater 2022;8(1):162. http://dx.doi.org/10.1038/s41524-022-00844-1.

[34] Mehnert M, Hossain M, Steinmann P. Towards a thermo-magneto-mechanical coupling framework for magneto-rheological elastomers. Int J Solids Struct 2017;128:117–32, URL https://www.sciencedirect.com/science/article/pii/S0020768317303864.

[35] Garcia-Gonzalez D, Hossain M. Microstructural modelling of hard-magnetic soft materials: Dipole–dipole interactions versus Zeeman effect. Extrem Mech Lett 2021;48:101382, URL https://www.sciencedirect.com/science/article/pii/S235243162100122X.

[36] Lucarini S, Moreno-Mateos MA, Danas K, Garcia-Gonzalez D. Insights into the viscohyperelastic response of soft magnetorheological elastomers: competition of macrostructural versus microstructural players. International Journal of Solids and Structures 2022;256:111981. http://dx.doi.org/10.1016/j.ijsolstr.2022.111981, https://www.sciencedirect.com/science/article/pii/S0020768322004346.

[37] Rambausek M, Mukherjee D, Danas K. A computational framework for magnetically hard and soft viscoelastic magnetorheological elastomers. Computer Methods in Applied Mechanics and Engineering 2022;391:114500. http://dx.doi.org/10.1016/j.cma.2021.114500, https://www.sciencedirect.com/science/article/pii/S0045782521007064.

[38] Utrera-Barrios S, Verdejo R, López-Manchado MA, Hernández Santana M. Evolution of self-healing elastomers, from extrinsic to combined intrinsic mechanisms: a review. Mater Horiz 2020;7:2882–902, URL http://dx.doi.org/10.1039/D0MH00535E.

[39] Guadagno L, Vertuccio L, Naddeo C, Calabrese E, Barra G, Raimondo M, et al. Self-healing epoxy nanocomposites via reversible hydrogen bonding. Composites B 2019;157:1–13, URL https://www.sciencedirect.com/science/article/pii/S1359836818313891.

[40] Song H, Sun Y, Zhu J, Xu J, Zhang C, Liu T. Hydrogen-bonded network enables polyelectrolyte complex hydrogels with high stretchability, excellent fatigue resistance and self-healability for human motion detection. Composites B 2021;217:108901, URL https://www.sciencedirect.com/science/article/pii/S1359836821002924.

[41] Fang Y, Xu J, Gao F, Du X, Du Z, Cheng X, et al. Self-healable and recyclable polyurethane-polyaniline hydrogel toward flexible strain sensor. Composites B 2021;219:108965, URL https://www.sciencedirect.com/science/article/pii/S135983682100353X.

[42] Jiang L, He S, Liu A, Zhang J, Liu J, He S, et al. Preparation and characterization of self-healable and wearable hydrogels with ultrasensitive sensing performances. Composites B 2022;239:109982, URL https://www.sciencedirect.com/science/article/pii/S1359836822003614.

[43] Cao Y, Wu H, Allec SI, Wong BM, Nguyen D-S, Wang C. A highly stretchy, transparent elastomer with the capability to automatically self-heal underwater. Adv Mater 2018;30(49):1804602, arXiv:https://onlinelibrary.wiley.com/doi/pdf/10.1002/adma.201804602, URL https://onlinelibrary.wiley.com/doi/abs/10.1002/adma.201804602.